



# Symmetric fractal trees in three dimensions

R.M. Frongillo<sup>a</sup>, E. Lock<sup>b</sup>, D.A. Brown<sup>c,\*</sup>

<sup>a</sup> *Cornell University, Department of Mathematics, Ithaca, NY 14850, USA*

<sup>b</sup> *Hamilton College, Department of Mathematics, Clinton, NY 13323, USA*

<sup>c</sup> *Ithaca College, Department of Mathematics, Ithaca, NY 14850, USA*

Accepted 10 April 2006

Communicated by Prof. G. Iovane

## Abstract

In this paper, we classify and describe a method for constructing fractal trees in three dimensions. We explore certain aspects of these trees, such as space-filling and self-contact.

© 2006 Published by Elsevier Ltd.

## 1. Introduction

A fractal tree can be loosely defined as a trunk and a number of branches that each look like the tree itself, thus creating a self-similar object. Often, these appear strikingly similar to real trees, and hence are used frequently as tree models. Fractal tree models have also been used in other areas, such as antenna construction [1] and mantle melting [2]. Many other applications of the structure of fractal trees are found in [5–9].

Mathematically, these trees have been studied primarily by Mandelbrot and Frame [3,4], who proved and conjectured properties of symmetric binary fractal trees in the plane. Mandelbrot and Frame looked into plane-filling trees, the shape of the canopy (or tip set), and conditions for self-contacting trees.

Less work has been done concerning fractal trees in three dimensions. Recent work in three dimensions has been initiated by Tancheva, Baker, and Maceli as part of the Research Experience for Undergraduates program at Ithaca College. These students developed a method for constructing and visualizing 3-branch trees. They also made conjectures about the shape of the canopy when a tree has tip-to-tip self-contact.

We continue to generalize the work of Mandelbrot and Frame to three dimensions. We show that the canopy of a tree with tip-to-tip self-contact forms a continuous surface, and give conditions for generating these trees. In addition, we discuss skew trees, a new class of fractal trees, and construct space-filling trees that fill boxes in arbitrarily many dimensions.

Finally, we mention that the search for scaling that results in tip-to-tip contact involves rather interesting constants, depending, of course, on the branching angles. In 2-dimensional trees with two branchings at angle of  $\pi/3$ , we see that the required scaling ratio turns out to be  $1/\phi$ , where  $\phi = \frac{1+\sqrt{5}}{2}$  is the Golden Ratio [3]. We see this same scaling ratio

\* Corresponding author.

E-mail addresses: [rmf25@cornell.edu](mailto:rmf25@cornell.edu) (R.M. Frongillo), [elock@hamilton.edu](mailto:elock@hamilton.edu) (E. Lock), [dabrown@ithaca.edu](mailto:dabrown@ithaca.edu) (D.A. Brown).

required in 3-dimensional trees when the branching angle is  $\arccos(-1/\sqrt{3})$ ; see Section 5. The appearance of the Golden Mean in the study of fractals and Hausdorff dimension can be found in several references [10–12].

**2. Fractal trees**

First, let us define a fractal tree more rigorously. We can do this with three parameters:

**Definition 2.1 (Fractal tree).** We denote a 3-dimensional fractal tree by  $\mathcal{T} = (r, \varphi, b)$ , where  $r$  is the scaling ratio at each level,  $\varphi$  is the angle of rotation in the  $y - z$  plane, and  $b$  is the number of branches.

With these parameters, we can construct the tree using affine transformations (functions of the form  $f(\vec{x}) = A\vec{x} + \vec{b}$ ).

**Definition 2.2 (Tree transformations).** For a fractal tree  $\mathcal{T} = (r, \varphi, b)$ , the corresponding affine transformations are

$$T_j(\vec{x}) = \vec{t} + r \begin{bmatrix} \cos(\theta_j) & -\sin(\theta_j) & 0 \\ \sin(\theta_j) & \cos(\theta_j) & 0 \\ 0 & 0 & 1 \end{bmatrix} \begin{bmatrix} 1 & 0 & 0 \\ 0 & \cos(\varphi) & -\sin(\varphi) \\ 0 & \sin(\varphi) & \cos(\varphi) \end{bmatrix} \vec{x},$$

where  $\theta_j = 2\pi(j - 1)/b$  and  $1 \leq j \leq b$ . The trunk  $\vec{t}$  of the tree is assumed throughout to be the standard vector

$$\vec{e}_3 = \begin{bmatrix} 0 \\ 0 \\ 1 \end{bmatrix}.$$

These transformations map the tip of a branch to the tips of its child branches: they scale the branch tip by  $r$ , rotate it about the  $x$ -axis by an angle  $\varphi$ , rotate it about the  $z$ -axis by an angle  $\theta_j$ , and finally translate it 1 unit in the  $z$  direction (see Fig. 1).

Skew trees, another class of fractal trees, are constructed in the same manner as the regular fractal tree, but with an additional rotation about the trunk at every level of the tree.

**Definition 2.3 (Skew tree).** We will denote by  $\mathcal{T}_{\text{skew}} = (r, \varphi, b)_S$  a skew tree, which has the same transformations as in Definition 2.2 except with  $\theta_j = 2\pi(j - \frac{1}{2})/b$  instead of  $2\pi(j - 1)/b$ .

With the transformations defined above, we define a path in the tree which we use to refer to specific parts of the tree. Paths are given by sequences of transformations.

**Definition 2.4 (Path).** Given a fractal tree  $\mathcal{T} = (r, \varphi, b)$ , a path  $p$  in  $\mathcal{T}$  is a string of integers  $s_1 s_2 \cdots s_k$ , where  $1 \leq s_i \leq b$ . The size of the path  $p$ , denoted  $|p|$ , is the number of integers,  $k$ . The tip of  $p$ ,  $\text{tip}(p)$ , is defined as

$$T_{s_1} \circ T_{s_2} \circ \cdots \circ T_{s_k}(\vec{e}_3).$$

It should be noted that paths in a tree are constructed somewhat counter-intuitively, since the first integer in the path corresponds to the outermost transformation, and the last integer to the innermost transformation. Fig. 1 shows the construction of the  $(\frac{2}{3}, \frac{\pi}{4}, 3)$  tree. Observe how each step contains three exact copies of the previous step coming out of the new trunk. This is the reason for the “inverted” paths; the transformations push points from the trunk toward the tips, so the tip of each path must correspond be the first transformation.

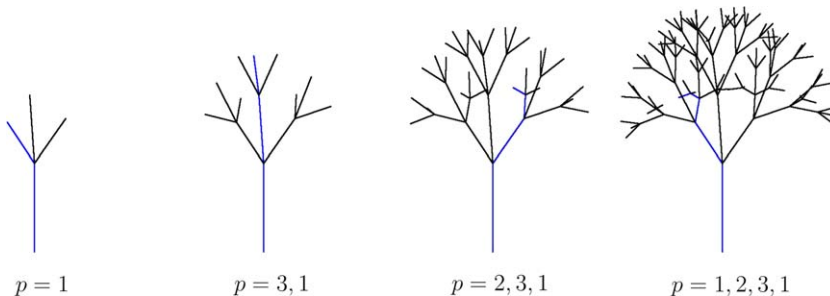


Fig. 1. The construction of the  $\mathcal{T} = (\frac{2}{3}, \frac{\pi}{4}, 3)$  fractal tree, and a path  $p$  in  $\mathcal{T}$ .

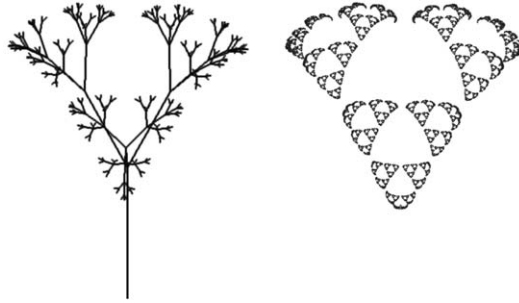


Fig. 2. The tip set of the  $(\frac{1}{2}, \frac{2}{6}, 3)$  tree, which resembles the Sierpinski triangle.

The main object of study of this paper is the tip set of a fractal tree, which is defined below, and illustrated in Fig. 2.  $\mathcal{H}$  denotes the space of compact subsets of  $\mathbb{R}^3$  with the Hausdorff metric.

**Definition 2.5** (*Tip set*). Let  $\mathcal{T} = (r, \varphi, b)$  be a fractal tree. The *tip set* or *canopy* of  $\mathcal{T}$ , denoted  $\text{tip}(\mathcal{T})$ , is the attractor of the iterated function system  $\{T_1, \dots, T_b\}$ . Thus,  $\text{tip}(\mathcal{T})$  is the fixed point of the function  $F: \mathcal{H} \rightarrow \mathcal{H}$ , where  $F(S) = T_1(S) \cup \dots \cup T_b(S)$ :

$$F(\text{tip}(\mathcal{T})) = \bigcup_{i=1}^b T_i(\text{tip}(\mathcal{T})) = \text{tip}(\mathcal{T}).$$

Our primary concerns regarding the tip set are the conditions under which a tree touches itself at the tips. This is the notion of (tip-to-tip) self-contact.

**Definition 2.6** (*Self-contact*). If two branches of a tree  $\mathcal{T}$  intersect,  $\mathcal{T}$  is said to have *self-contact*. If branches of  $\mathcal{T}$  intersect only at the tips ( $\text{tip}(p) = \text{tip}(q)$  for distinct paths  $p, q \in \mathcal{T}$ ),  $\mathcal{T}$  is said to have *tip-to-tip self-contact*.

Note that by symmetry and self-similarity, if two branches intersect, then the tree self-contacts infinitely many times. Similarly, if a tree has tip-to-tip self-contact, the tip set will be connected and form a continuous curve, as we show in the next section.

### 3. Connectedness of a self-contacting canopy

Here we show that the canopy of a tree with tip-to-tip self-contact is connected, and therefore forms a continuous curve.

**Definition 3.1** ( $\epsilon$ -Connected). A set  $S$  is  $\epsilon$ -connected if for any two points  $x, y \in S$  there is a finite sequence of points  $s_1, s_2, \dots, s_n \in S$  such that  $s_1 = x$ ,  $s_n = y$ , and  $\|s_i - s_{i+1}\| < \epsilon$  for all  $1 \leq i < n$ . Such a finite sequence is called an  $\epsilon$ -chain from  $x$  to  $y$ .

**Lemma 3.2** ( $\epsilon$ -Connectedness of contractions). Let  $f: X \rightarrow Y$  be a contractive mapping with Lipschitz constant  $r < 1$ . Then if  $S \subseteq X$  is  $\epsilon$ -connected,  $f(S)$  is  $r\epsilon$ -connected.

**Proof.** Let  $x, y$  be any two points in  $S$ . By Definition 3.1, we can find an  $\epsilon$ -chain  $s_1, \dots, s_n$  from  $x$  to  $y$  such that  $\|s_i - s_{i+1}\| < \epsilon$  for all  $1 \leq i < n$ . Since  $f$  is a contraction, we then have that  $\|f(s_i) - f(s_{i+1})\| \leq r\|s_i - s_{i+1}\| < r\epsilon$ , so  $f(s_1), \dots, f(s_n)$  is an  $r\epsilon$ -chain from  $f(x)$  to  $f(y)$ . Since we can pick  $x, y$  such that  $f(x), f(y) \in f(S)$  are arbitrary,  $f(S)$  must be  $r\epsilon$ -connected.  $\square$

**Theorem 3.3** (Connectedness of the attractor of an IFS). Let  $A$  be the attractor of the iterated function system  $\{T_1, \dots, T_n\}$ , where each  $T_i$  is a contractive homeomorphism with Lipschitz constant  $r < 1$ . Let  $G$  be the graph with vertices  $V = \{T_i\}$  and edges  $E = \{(T_i, T_j) \mid T_i(A) \cap T_j(A) \neq \emptyset\}$ . Then  $A$  is connected if and only if  $G$  is connected.

**Proof.** Assume  $A$  is connected. Then as each  $T_i$  is continuous,  $T_i(A)$  is also connected. If we also assume that  $G$  is not connected, then there exists a nonempty set  $S \subsetneq V$  such that there are no edges  $(s, v) \in E$  with  $s \in S$  and  $v \in V - S$ . Thus,  $T_i(A) \cap T_j(A) = \emptyset$  for all  $T_i \in S$  and  $T_j \in V - S$ . We now define sets  $C$  and  $D$  as follows:

$$C = \bigcup_{T_i \in S} T_i(A), \quad D = \bigcup_{T_j \in V-S} T_j(A).$$

Note that  $C$  and  $D$  are disjoint, but  $C \cup D = T_1(A) \cup \dots \cup T_n(A) = A$ . Since each  $T_i$  is a homeomorphism and  $A$  is closed, we have that each  $T_i(A)$  is closed, and thus  $C$  and  $D$  are closed as finite unions of closed sets. Thus  $A$  must be disconnected, which is a contradiction.

Assume that  $A$  is disconnected but  $G$  is connected. We can then find disjoint closed sets  $C, D$  such that  $C \cup D = A$ . As  $C$  and  $D$  are disjoint there must be some nonzero distance between them,  $\delta$ . If we let  $d$  be the diameter of  $A$ , we trivially have that  $A$  is  $d$ -connected. By Lemma 3.2, since each  $T_i$  has a Lipschitz constant  $r < 1$ , we have that  $T_i(A)$  is  $rd$ -connected. We now show that  $F(A)$  is  $rd$ -connected, where  $F(A) = T_1(A) \cup \dots \cup T_n(A)$ .

Let  $x \in T_i(A)$  and  $y \in T_j(A)$  be any two points in  $F(A)$ , and let  $T_{a_1}, \dots, T_{a_k}$  be a path in  $G$  from  $T_{a_1} = T_i$  to  $T_{a_k} = T_j$ . Since  $T_{a_i} \cap T_{a_{i+1}}$  is nonempty for all  $i < k$  (by definition of  $G$ ), we can define points  $s_1, \dots, s_{k-1}$ , where each  $s_i \in T_{a_i} \cap T_{a_{i+1}}$ . We can now build a giant  $rd$ -chain from  $x$  to  $y$ , since there is an  $rd$ -chain between  $x$  and  $s_1$ , between each  $s_i$  and  $s_{i+1}$ , and between  $s_{k-1}$  and  $y$ . Therefore,  $F(A) = A$  is  $rd$ -connected.

We can continue this process indefinitely, so that  $F^m(A) = A$  is  $r^m d$ -connected. Since  $r < 1$  there must be some  $m$  for which  $r^m d < \delta$ , but this is a contradiction since  $C$  and  $D$  are separated by  $\delta$ .  $\square$

**Theorem 3.4** (Attractors and curves). *Let  $A$  be the attractor of an IFS  $\{T_1, \dots, T_n\}$  such that each  $T_i$  is a contractive homeomorphism with Lipschitz constant  $r < 1$ . Then  $A$  is path-connected and a continuous image of  $[0, 1]$ .*

**Proof.** By Theorem 3.3,  $A$  is connected. We now show that  $A$  is locally connected.

Let  $x \in A$  be arbitrary. Since  $A = \cup T_i(A)$ , there must be some  $i$  for which  $x \in T_i(A)$ . We can also find  $j$  for which  $x \in T_i \circ T_j(A)$ , since  $T_i(A) = \cup T_j \circ T_i(A)$ . Continuing this process, we obtain an infinite sequence  $\{s_i\}$  such that  $x \in F(k)$  for all  $k$ , where  $F(k) = T_{s_1} \circ T_{s_2} \circ \dots \circ T_{s_n}(A)$ . Now, since  $A \in \mathcal{H}$  is compact, and thus closed and bounded as a subset of  $\mathbb{R}^n$ , there must be some finite diameter  $d$  of  $A$ . Since each  $T_i$  have a Lipschitz constant  $r < 1$ , we now have that  $F(k)$  has diameter  $r^k d$  for all  $k$ , and is connected since  $A$  is connected. Thus,  $x$  is in an arbitrarily small connected subset of  $A$ , and since  $x$  was arbitrary,  $A$  is locally connected.

We now have by the Hahn–Mazurkiewicz theorem that  $A$  is a continuous image of the interval  $[0, 1]$  and thus is a curve.  $\square$

The corollary below follows immediately from Theorem 3.4, since the canopy of a fractal tree is the attractor of the tree’s transformations.

**Corollary 3.5** (Canopies and curves). *If a fractal tree  $\mathcal{T}$  has tip-to-tip self-contact, its canopy tip ( $\mathcal{T}$ ) will be connected, locally connected, and a curve.*

#### 4. Approximating conditions for self-contact

Given branching angle  $\varphi$ , we outline the method used to compute the value of  $r$  required for tip-to-tip self-contact in a symmetric fractal tree. In other words, our method determines the greatest scaling ratio possible without a given tree intersecting itself.

Note that by self-similarity, it is enough to determine the conditions for contact between the first and second original branches (the branches generated by  $T_1$  and  $T_2$ , respectively). By symmetry, the two branches will intersect if and only if the tree created from the first branch crosses the plane bisecting these two branches (see Fig. 3).

To find the correct ratio for a given angle  $\varphi$ , we first determine the path along the branches that moves toward this plane the fastest (as explained below). Although this path must follow an infinite number of branches, it is easy to compute up to a specified length. Our program, written in *Matlab*, takes  $\varphi$ , the number of branches, and the path size, then searches for the sequence of branch transformations (starting at branch 1) that moves the greatest distance in the direction of the bisecting plane.

After determining this path up to a certain length, we can search for the scaling ratio that brings the tip of the path closest to the plane. If our path length is reasonably long, this should provide a very precise approximation for the ratio required for tip-to-tip self-contact in the infinite case.

This method is useful in comparing the ratios required for tip-to-tip self-contact among trees with different numbers of branches and different  $\varphi$  values. Generally, we have found that as the number of branches in the tree increases, the ratio decreases. As a function of  $\varphi$ , the ratio typically follows a continuous curve. This curve changes dramatically at certain values of  $\varphi$ , however, which we will discuss in the next section.

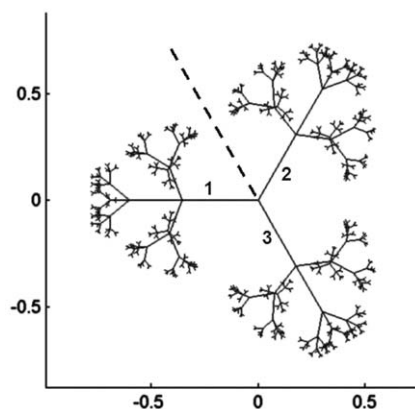


Fig. 3. A top down view of a 3-branch tree. The dotted line represents the plane bisecting branches 1 and 2.

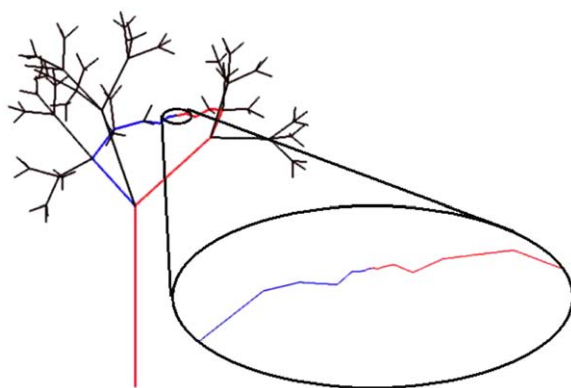


Fig. 4. A 3-branch tree with  $\varphi = \pi/4$  and  $r = .5507$ , conditions that should approximate tip-to-tip self-contact. The first 20 transformations of the path starting at the first branch are drawn in blue, and its symmetric complement is drawn in red. As illustrated, they come very close to connecting at the tips. (For interpretation of the references to color in this figure legend, the reader is referred to the web version of this article.)

This method can also be used to find and compare self-contact ratios among skew trees. Typically, these ratios will vary significantly from that of their non-skew counterparts (see Figs. 4 and 5).

## 5. Mathematical results involving conditions for self-contact

When looking at the paths giving us tip-to-tip self-contact, three things become apparent. First, the same path often works for a wide range of  $\varphi$  values. Second, the paths typically change at critical points in the  $r$ - $\varphi$  plot. And third, paths typically end with an infinite sequence of the same transformation. These three characteristics are helpful in uncovering mathematical expressions for the conditions of self-contact.

In the four branch case, the path 1213 seems to work for  $\varphi \approx 1.27$  rad to  $\varphi \approx 2.00$ . During this interval, the  $r$ - $\varphi$  plot forms a smooth curve. Then, when  $\varphi \approx 2.00$ , the path changes to 1243 and the  $r$ - $\varphi$  plot abruptly changes direction. We can find exactly where this change occurs, then, by solving for when the path 124 brings us closer to the plane bisecting the first two branches than 121. This happens to occur precisely at  $\varphi = \arccos(1 - \sqrt{2})$ . This method can be used to find exactly where the  $r$ - $\varphi$  plot changes in many cases (see Fig. 6 and Fig. 7).

In the four branch case,  $\varphi = \arccos(1 - \sqrt{2})$  happens to give the maximum ratio for tip-to-tip self-contact. Trees with a different number of branches also typically have their maximum ratio at a point where the path changes significantly, allowing us to solve for  $\varphi$  at this point.

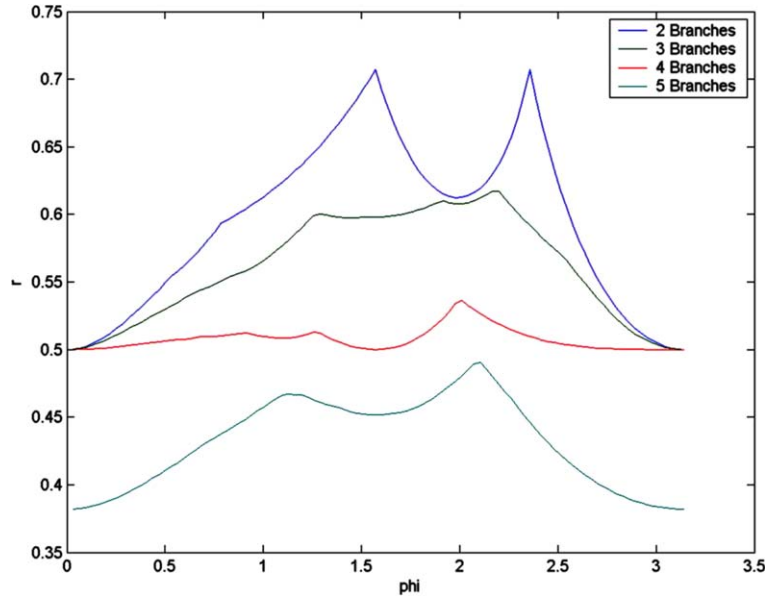


Fig. 5. An  $r$ - $\phi$  plot for 2, 3, 4 and 5 branch trees. The two branch plot at the top is identical to that found by Mandelbrot and Frame in the planar case [3].

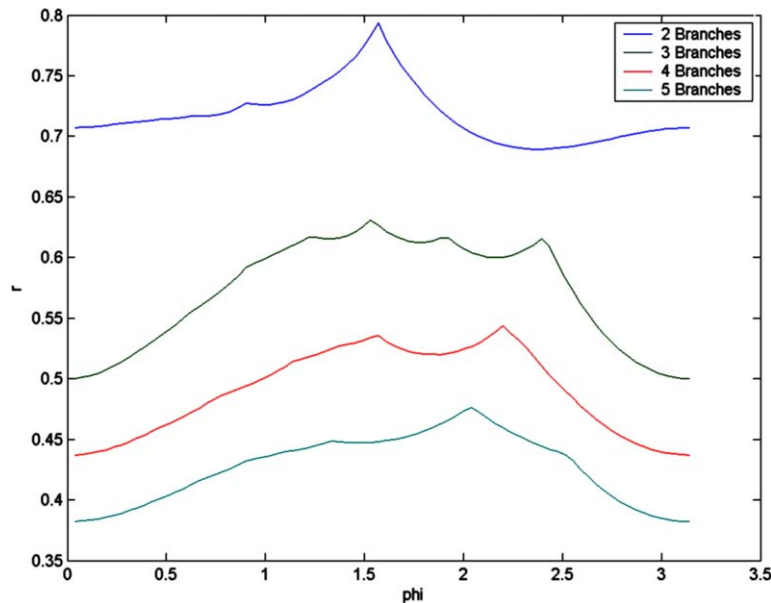


Fig. 6. An  $r$ - $\phi$  plot for skew 2, 3, 4 and 5 branch trees.

In Table 1, we give precise mathematical expressions for the maximum scaling ratios in the 2, 4 and 6 branch cases. Here, we have been able to find closed formulas for the point at the tip of the infinite path (that is, the path of infinite size). When the dot product of this point and the normal to the plane bisecting branches 1 and 2 is equal to zero, this point will lie on the plane. Hence, we can solve for the correct scaling ratio. Using this method, we have found  $r$ - $\phi$  equations yielding tip-to-tip self-contact for 4 branch, 6 branch, skew 3 and skew 5 branch trees. Our equations, along with the paths giving us self-contact, are included in Table 2 for the skew 3-branch trees; for shorthand we define

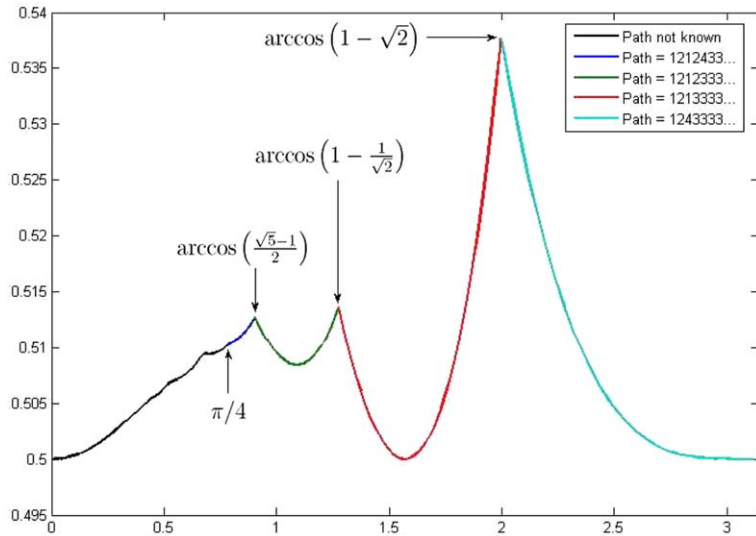


Fig. 7. Path changes in the 4-branch tree. Note that  $\varphi = \arccos(1 - \sqrt{2})$  gives the maximum value of  $r$ .

Table 1  
Maximum branching ratios

Branches	Expression for $\varphi$	Expression for $r$	Approximation of $r$
2	$\arccos(\frac{-1}{\sqrt{2}}), \frac{\pi}{2}$	$\frac{1}{\sqrt{2}}$	0.707
3	$\arccos(\frac{-1}{\sqrt{3}})$		0.619
4	$\arccos(1 - \sqrt{2})$	$\frac{-1 + \sqrt{-3 + 4\sqrt{2}}}{4 - 2\sqrt{2}}$	0.538
5	$\arccos\left(1 - 2\sqrt{1 - \frac{1}{\sqrt{5}}}\right)$		0.490
6	$\arccos(\frac{3 - \sqrt{33}}{6})$	$\frac{3 + \sqrt{33} - \sqrt{114 - 2\sqrt{33}}}{-9 + \sqrt{33}}$	0.424

Table 2  
Paths and equations that determine self-contact in 3 branch skew trees

$\varphi$ Interval	Path	Equation determining self-contact
$[\arccos(\frac{2\sqrt{3}-1}{3}), \arccos(\frac{2\sqrt{2}-1}{3})]$	123132	$-8 + r^2(16 + (4 - 5r)r) + 12r^3(1 + r)\cos\varphi + 9r^4\cos(2\varphi) = 0$
$[\arccos(\frac{2\sqrt{2}-1}{3}), \arccos(\frac{1}{3})]$	12312	$-2 + r^2(4 + r) + 3r^3\cos\varphi = 0$
$[\arccos(\frac{1}{3}), \alpha]$	11132	$-32 + 16r + 20r^2 + 14r^3 + (-48r + 48r^2 + 27r^3)\cos\varphi + (-12r + 6r^2)\cos(2\varphi) - 9r^2\cos(3\varphi) = 0$
$[\alpha, \arccos(-\frac{1}{3})]$	1112	$r = \frac{-2 + 6\cos\varphi + \sqrt{62 + 72\cos\varphi - 54\cos(2\varphi)}}{5 + 12\cos\varphi - 9\cos(2\varphi)}$
$[\arccos(-\frac{1}{3}), \arccos(-\frac{\sqrt{5}}{3})]$	1132	$r = \frac{2}{1 - 3\cos\varphi}$

$$\alpha = \frac{1}{9} \left( 1 - 2\sqrt{7} \left( \cos \left( \frac{\arctan(3\sqrt{3})}{3} \right) + \sqrt{3} \sin \left( \frac{\arctan(3\sqrt{3})}{3} \right) \right) \right)$$

### 6. Space-filling trees

To find a fractal tree that fills space, we must first define exactly what we are looking for. Below are definitions of dimension and of space-filling.

**Definition 6.1 (Hausdorff dimension).** The Hausdorff dimension  $d$  of a fractal tree  $\mathcal{T} = (r, \varphi, b)$  or  $\mathcal{T} = (r, \varphi, b)_S$  is given by the formula

$$d = \frac{\ln b}{\ln \frac{1}{r}}$$

**Definition 6.2** (*Space-filling*). A fractal tree  $\mathcal{T}$  fills  $n$ -dimensional space if

$$\prod_{i=1}^n [a_i, b_i] \subset \text{tip}(\mathcal{T})$$

for  $a_i < b_i$ , and  $\prod$  denotes the cartesian product.

These definitions are not as similar as one might think. It is not enough for a tree to simply be  $n$ -dimensional for it to fill  $n$ -dimensional space; it must also contain a closed box in  $n$ -dimensional space. The reason for this is that if the tree overlaps itself significantly, the Hausdorff dimension would count many points more than once (by self-similarity, infinitely many). Fig. 8 shows a skew, 2-branch tree that illustrates this difference.

The tree  $\mathcal{T}$  we are looking for is also a skew, 2-branch fractal tree, with the same scaling ratio of  $1/\sqrt[3]{2}$ , since we want the Hausdorff dimension to be 3. The parameter that we must change is  $\varphi$ . It turns out that  $\mathcal{T}$  fills space when  $\varphi$  is a right angle, so  $\mathcal{T} = (1/\sqrt[3]{2}, \frac{\pi}{2}, 2)_S$ .  $\mathcal{T}$  has the following simple transformations:

$$T_1(\vec{x}) = \begin{bmatrix} 0 & 0 & r \\ r & 0 & 0 \\ 0 & r & 0 \end{bmatrix} \vec{x} + \begin{bmatrix} 0 \\ 0 \\ 1 \end{bmatrix}$$

$$T_2(\vec{x}) = \begin{bmatrix} 0 & 0 & -r \\ -r & 0 & 0 \\ 0 & r & 0 \end{bmatrix} \vec{x} + \begin{bmatrix} 0 \\ 0 \\ 1 \end{bmatrix}.$$

Fig. 9 shows  $\mathcal{T}$  and its canopy, which seems to fill up a box. To prove this, however, we need to start by proving properties of a simple set of sequences.

**Definition 6.3** (*The  $L$  set*). Let  $L$  be the set given by the sequence  $1 + \frac{1}{2} + \frac{1}{4} + \dots$  with every possible combination of signs. That is,

$$L = \left\{ \sum_{n=0}^{\infty} \frac{\sigma_n}{2^n} \mid \sigma_n \in \{-1, 1\} \right\}.$$

**Lemma 6.4** (*Properties of  $L$* ).

- (a)  $\{-l \mid l \in L\} = L$
- (b)  $\{1 + l/2 \mid l \in L\} \cup \{-1 + l/2 \mid l \in L\} = L$

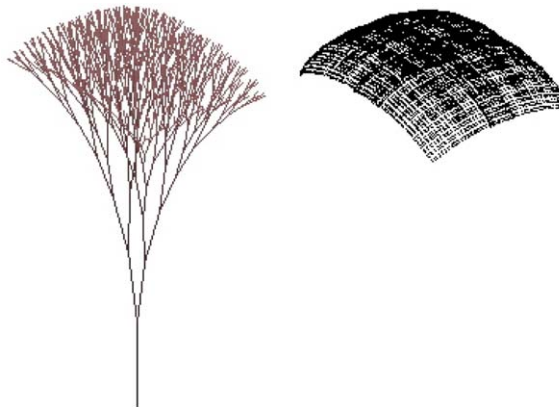


Fig. 8. A “3-dimensional” tree with parameters  $(1/\sqrt[3]{2}, \frac{\pi}{18}, 2)_S$ , and its tip set (to 15 iterations). The tree certainly does not fill 3-space, though it may fill a 2-dimensional surface.

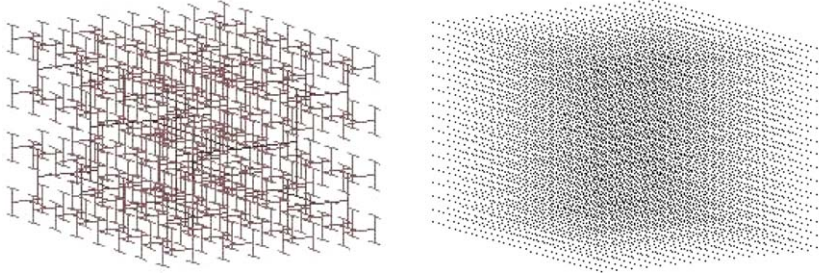


Fig. 9. A space-filling tree.

**Proof**

- (a) For any  $l \in L$ ,  $-l$  is given by switching the sign of each  $\sigma_n$ . Thus,  $-l \in L$ . Since negation is invertible ( $-(-l) = l$  for all  $l \in L$ ), we have trivially that  $-L = \{-l | l \in L\} = L$ .
- (a) Performing the union directly, we have

$$\begin{aligned} \{1 + l/2 | l \in L\} \cup \{-1 + l/2 | l \in L\} &= \left\{ 1 + \sum_{n=1}^{\infty} \frac{\sigma_n}{2^n} \mid \sigma_n \in \{-1, 1\} \right\} \cup \left\{ -1 + \sum_{n=1}^{\infty} \frac{\sigma_n}{2^n} \mid \sigma_n \in \{-1, 1\} \right\} \\ &= \left\{ \sigma_0 + \sum_{n=1}^{\infty} \frac{\sigma_n}{2^n} \mid \sigma_n \in \{-1, 1\} \right\} = \left\{ \sum_{n=0}^{\infty} \frac{\sigma_n}{2^n} \mid \sigma_n \in \{-1, 1\} \right\} = L \end{aligned}$$

Though it may not be apparent,  $L$  is just a closed interval on the real line.  $\square$

**Lemma 6.5** (Equivalent expression of  $L$ ).  $L = [-2, 2]$ .

**Proof.** Let  $x$  be any real number in the interval  $[0, 2]$  and let  $b_0 \cdot b_1 b_2 b_3 \dots$  be a binary representation of  $x$ . We can also write  $x = s_0 s_1 s_2 s_3 \dots$  or  $x = s_0 s_1 s_2 \dots s_{m-1} s_m^*$ , where each  $s_i = 000 \dots 01$ , and  $s_i^* = 000 \dots$  (with an implicit decimal point after the first digit of  $s_0$  or  $s_0^*$ ). Note that it is possible for  $s_i$  to be the string consisting of a solitary 1. We now find an element  $l$  of  $L$  such that  $l = x$ .

For each  $s_i = b_{J_i} b_{J_i+1} \dots b_{J_i+K_i}$  set  $\sigma_{J_i} = 1$  and  $\sigma_{J_i+1} \dots \sigma_{J_i+K_i} = -1$ , where  $K_i = J_{i+1} - J_i - 1$ . If in the second case, and the repeating zeros start at position  $m$ , set  $\sigma_{J_m} = 1$  and  $\sigma_{J_m+k} = -1$  for  $k \geq 1$ . We check that these assignments are equivalent at each step, first for  $s_i$ :

$$\begin{aligned} \sum_{n=J_i}^{J_i+K_i} \frac{b_n}{2^n} &= \frac{1}{2^{J_i}} \left( \frac{0}{1} + \frac{0}{2} + \frac{0}{4} + \dots + \frac{0}{2^{K_i-1}} + \frac{1}{2^{K_i}} \right) = \frac{1}{2^{J_i}} \left( \frac{1}{2^{K_i}} \right) = \frac{1}{2^{J_i+K_i}} \\ \sum_{n=J_i}^{J_i+K_i} \frac{\sigma_n}{2^n} &= \frac{1}{2^{J_i}} \left( \frac{1}{1} - \frac{1}{2} - \frac{1}{4} - \dots - \frac{1}{2^{K_i}} \right) = \frac{1}{2^{J_i}} \left( \frac{1}{2^{K_i}} \right) = \frac{1}{2^{J_i+K_i}}, \end{aligned}$$

and also for  $s_m^*$ :

$$\sum_{n=J_m}^{\infty} \frac{b_n}{2^n} = \sum_{n=J_m}^{\infty} 0 = 0; \quad \sum_{n=J_m}^{\infty} \frac{\sigma_n}{2^n} = \frac{1}{2^{J_m}} \left( 1 - \sum_{n=1}^{\infty} \frac{1}{2^n} \right) = \frac{1}{2^{J_m}} (0) = 0.$$

We now have the following:

$$\begin{aligned} x = s_0 s_1 s_2 \dots &= \sum_{n=0}^{\infty} \frac{b_n}{2^n} = \sum_{i=0}^{\infty} \sum_{n=J_i}^{J_i+K_i} \frac{b_n}{2^n} = \sum_{i=0}^{\infty} \sum_{n=J_i}^{J_i+K_i} \frac{\sigma_n}{2^n} = \sum_{n=0}^{\infty} \frac{\sigma_n}{2^n} = l \\ x = s_0 \dots s_{m-1} s_m^* &= \sum_{n=0}^{\infty} \frac{b_n}{2^n} = \sum_{i=0}^{m-1} \sum_{n=J_i}^{J_i+K_i} \frac{b_n}{2^n} = \sum_{i=0}^{m-1} \sum_{n=J_i}^{J_i+K_i} \frac{\sigma_n}{2^n} = \sum_{n=0}^{\infty} \frac{\sigma_n}{2^n} = l. \end{aligned}$$

Clearly, for  $x \in [-2, 0]$ , we can use the above construction to find  $l = -x$  and simply negate every  $\sigma_n$  as discussed in Lemma 6.4.a, so that  $-l = x$ . Thus  $[-2, 2] \subseteq L$ .

Finally, for any  $l \in L$ ,

$$|l| = \left| \sum_{n=0}^{\infty} \frac{\sigma_n}{2^n} \right| \leq \sum_{n=0}^{\infty} \frac{|\sigma_n|}{2^n} = \sum_{n=0}^{\infty} \frac{1}{2^n} = 2,$$

so  $L \subseteq [-2, 2]$ . Therefore,  $L = [-2, 2]$ .  $\square$

With this background in place, we can show that  $\mathcal{F}$  fills space.

**Theorem 6.6** (Space-filling tree). *Let  $S^*$  be the tip set of the fractal tree  $\mathcal{F}$  with  $\varphi = \pi/2$  and  $r = 1/\sqrt[3]{2}$ . Then*

$$S^* = [-\sqrt[3]{4}, \sqrt[3]{4}] \times [-\sqrt[3]{2}, \sqrt[3]{2}] \times [0, 2].$$

**Proof.** By Definition 2.5, the tip set  $S^*$  is defined as the attractor of the iterated function system  $\{T_1, T_2\}$ . This we can check by showing that  $S^*$  is a fixed point of the set-valued function  $F(S) = T_1(S) \cup T_2(S)$ , or in other words, that  $F(S^*) = S^*$ . We first show that

$$S^* = \left\{ \left[ \begin{array}{c} rl_x \\ r^2 l_y \\ 1 + r^3 l_z \end{array} \right] \middle| l_x, l_y, l_z \in L \right\},$$

which we can do directly using Lemma 6.4:

$$F(S^*) = \left\{ \left[ \begin{array}{c} r(1 + r^3 l_z) \\ r(rl_x) \\ 1 + r(r^2 l_y) \end{array} \right] \middle| l_x \in L \right\} \cup \left\{ \left[ \begin{array}{c} -r(1 + r^3 l_z) \\ -r(rl_x) \\ 1 + r(r^2 l_y) \end{array} \right] \middle| l_x \in L \right\} \tag{1}$$

$$= \left\{ \left[ \begin{array}{c} r(1 + r^3 l_x) \\ r^2 l_y \\ 1 + r^3 l_z \end{array} \right] \middle| l_x \in L \right\} \cup \left\{ \left[ \begin{array}{c} r(-1 - r^3 l_x) \\ -r^2 l_y \\ 1 + r^3 l_z \end{array} \right] \middle| l_x \in L \right\} \tag{2}$$

$$= \left\{ \left[ \begin{array}{c} r(1 + \frac{1}{2} l_x) \\ r^2 l_y \\ 1 + r^3 l_z \end{array} \right] \middle| l_x \in L \right\} \cup \left\{ \left[ \begin{array}{c} r(-1 + \frac{1}{2} l_x) \\ r^2 l_y \\ 1 + r^3 l_z \end{array} \right] \middle| l_x \in L \right\} \tag{3}$$

$$= \left\{ \left[ \begin{array}{c} rl_x \\ r^2 l_y \\ 1 + r^3 l_z \end{array} \right] \middle| l_x, l_y, l_z \in L \right\} = S^*, \tag{4}$$

where (2) was obtained by renaming, (3) by Lemma 6.4.a and the definition of  $r$ , and (4) by Lemma 6.4.b.

Finally, by Lemma 6.5, we have

$$S^* = [-2r, 2r] \times [-2r^2, 2r^2] \times [1 - 2r^3, 1 + 2r^3] = [-\sqrt[3]{4}, \sqrt[3]{4}] \times [-\sqrt[3]{2}, \sqrt[3]{2}] \times [0, 2]. \quad \square$$

We can also find a tree  $\mathcal{F}_n$  that fills  $n$ -dimensional space. First, we must generalize the notion of a fractal tree.

**Definition 6.7** (Higher dimensional fractal tree). We denote an  $n$ -dimensional fractal tree by  $\mathcal{F} = (r, \varphi_2, \varphi_3, \dots, \varphi_{n-1}, b)$ , or  $(\dots)_S$ , where  $r$  and  $b$  are as defined previously, and  $\varphi_i$  is the angle of rotation in the plane of coordinates  $i$  and  $i + 1$ .

It may be confusing for  $\{\varphi_i\}$  to start with  $i = 2$ , but this is because  $b$  still determines the  $\theta$  values, which are rotations in the plane of coordinates 1 and 2.

**Definition 6.8** (Generalized tree transformations). For an  $n$ -dimensional fractal tree  $\mathcal{F} = (r, \varphi_2, \varphi_3, \dots, \varphi_{n-1}, b)$ , the corresponding affine transformations are

$$T_j(\vec{x}) = R_{1,2}(\theta_j) \cdot R_{2,3}(\varphi_2) \cdots R_{n-1,n}(\varphi_{n-1}) + \vec{e}_n$$

where  $\theta_j = 2\pi(j - 1)/b$ , or  $2\pi(j - \frac{1}{2})/b$  if  $\mathcal{F}$  is skew, and  $1 \leq j \leq b$ .

Using these definitions, we can find a tree  $\mathcal{F}_n$  that fills  $n$ -dimensional space.

**Theorem 6.9** (Space-filling tree in  $n$  dimensions).

Let  $\mathcal{T}_n = (\frac{1}{\sqrt{2}}, \frac{\pi}{2}, \dots, \frac{\pi}{2}, 2)_S$ . Then

$$\text{tip}(\mathcal{T}_n) = \left( \prod_{i=1}^{n-1} \left[ -\sqrt[n]{2^{n-i}}, \sqrt[n]{2^{n-i}} \right] \right) \times [0, 2].$$

**Proof.** First, we must figure out the transformations for  $\mathcal{T}_n$ . This is not hard due to all the right angles:

$$R_{i,i+1}\left(\frac{\pi}{2}\right) = \begin{bmatrix} I_{i-1} & 0 & 0 \\ 0 & \begin{bmatrix} 0 & -1 \\ 1 & 0 \end{bmatrix} & 0 \\ 0 & 0 & I_{n-i-1} \end{bmatrix}, \tag{5}$$

so we have that

$$T_1(\vec{x}) = r \begin{bmatrix} 0 & \dots & 0 & 1 \\ 1 & 0 & \dots & 0 \\ 0 & 1 & \ddots & \vdots \\ \vdots & \ddots & \ddots & 0 \\ 0 & \dots & 0 & 1 \end{bmatrix} + \begin{bmatrix} 0 \\ 0 \\ \vdots \\ 0 \\ 1 \end{bmatrix} \tag{6}$$

$$T_2(\vec{x}) = r \begin{bmatrix} 0 & \dots & 0 & 0 & -1 \\ -1 & 0 & \dots & 0 & 0 \\ 0 & 1 & 0 & \dots & 0 \\ \vdots & \ddots & \ddots & \ddots & \vdots \\ 0 & \dots & 0 & 1 & 0 \end{bmatrix} + \begin{bmatrix} 0 \\ 0 \\ \vdots \\ 0 \\ 1 \end{bmatrix}. \tag{7}$$

The proof from this point on is similar to that of [Theorem 6.6](#). We again define  $S_n^* = \text{tip}(\mathcal{T}_n)$  and express  $S_n^*$  in terms of elements of  $L$ :

$$S_n^* = \left\{ \left[ \begin{array}{c} rl_1 \\ r^2l_2 \\ \vdots \\ r^{n-1}l_{n-1} \\ 1 + r^n l_n \end{array} \right] \middle| l_i \in L \right\}.$$

We can again show this directly with [Lemma 6.4](#):

$$F(S_n^*) = \left\{ \left[ \begin{array}{c} \sigma r(1 + r^n l_n) \\ \sigma r(rl_1) \\ r(r^2l_2) \\ \vdots \\ r(r^{n-2}l_{n-2}) \\ 1 + r(r^{n-1}l_{n-1}) \end{array} \right] \middle| \begin{array}{l} l_i \in L, \\ \sigma \in \{-1, 1\} \end{array} \right\} \tag{8}$$

$$= \left\{ \left[ \begin{array}{c} r(\sigma + \frac{1}{2}l_n) \\ r^2l_1 \\ \vdots \\ r^{n-1}l_{n-2} \\ 1 + r^n l_{n-1} \end{array} \right] \middle| \begin{array}{l} l_i \in L, \\ \sigma \in \{-1, 1\} \end{array} \right\} \tag{9}$$

$$= \left\{ \left[ \begin{array}{c} r(l_1) \\ r^2 l_2 \\ \vdots \\ r^{n-1} l_{n-1} \\ 1 + r^n l_n \end{array} \right] \middle| \begin{array}{l} l_i \in L, \\ \sigma \in \{-1, 1\} \end{array} \right\} = S_n^* \quad (10)$$

where (9) was obtained by Lemma 6.4.a and the definition of  $r$ , and 4 by Lemma 6.4.b and then renaming the  $l_i$ .

We then have, by Lemma 6.5,

$$S^* = \left( \prod_{i=1}^{n-1} [-2r^i, 2r^i] \right) \times [0, 2] = \left( \prod_{i=1}^{n-1} [-\sqrt[n]{2^{n-i}}, \sqrt[n]{2^{n-i}}] \right) \times [0, 2]. \quad \square$$

## References

- [1] Petko JS, Werner DH. Miniature reconfigurable three-dimensional fractal tree antennas. *IEEE Trans Antennas Propag* 2004;52(8):1945–56.
- [2] Hart SR. Equilibration during mantle melting: a fractal tree model. *Proc Natl Acad Sci USA* 1993;90(24):11914–8.
- [3] Mandelbrot BB, Frame M. The canopy and shortest path in a self-contacting fractal tree – exactly what tangles the branches can get into. *Math Intelligencer* 1999;21(2):18.
- [4] Mandelbrot BB. *The fractal geometry of nature*. New York: Freeman; 1983 (2004).
- [5] Aris R. Diffusion and reaction in a Mandelbrot lung. *Chaos, Solitons & Fractals* 1991;1(6):583–93.
- [6] Sivakumar B. Chaos theory in geophysics: past present and future. *Chaos, Solitons & Fractals* 2004;19(2):441–62.
- [7] Gabryś E, Rybaczuk M, Kędzia A. Fractal models of circulatory system. *Chaos, Solitons & Fractals* 2005;24(3):707–15.
- [8] Abdusalam HA, Ahmed E. Modeling the failure of a fractal tree and Julia sets. *Chaos, Solitons & Fractals* 2000;11(13):2075–8.
- [9] Abdusalam HA. A probabilistic approach to the site percolation problems using fractal tree. *Chaos, Solitons & Fractals* 2000;11(9):1407–10.
- [10] El Naschie MS. Silver mean Hausdorff dimension and cantor sets. *Chaos, Solitons & Fractals* 1994;4(10):1861–70.
- [11] El Naschie MS. Dimensions and cantor spectra. *Chaos, Solitons & Fractals* 1994;4(11):2121–32.
- [12] Castro C. Fractal strings as an alternative justification for El Naschie’s cantorion spacetime and the fine structure constant. *Chaos, Solitons & Fractals* 2002;14(9):1341–51.